Biochimica et Biophysica Acta, 644 (1981) 333–340
Elsevier/North-Holland Biomedical Press

BBA 79288

AUTORADIOGRAPHIC LOCALISATION OF [^{3}H]OUABAIN BOUND TO CULTURED EPITHELIAL CELL MONOLAYERS OF MDCK CELLS

J.F. LAMB, P. OGDEN and N.L. SIMMONS

Department of Physiology and Pharmacology, University of St. Andrews, Fife, KY16 9TS (U.K.)

(Received December 22nd, 1980)

Key words: Cell culture; Ouabain localization; ($Na^+ + K^+$)-ATPase; Autoradiography; (MDCK cell)

[^{3}H]Ouabain binding to intact MDCK (cultured monolayers of dog kidney) cells of 60 serial passages is dependent upon ouabain concentration, time and medium K^+. By utilising high K^+ incubations to estimate non-specific [^{3}H]ouabain-binding, the concentration of ouabain giving half maximal specific binding was estimated to be $1.0 \cdot 10^{-7}$ M and the total maximum binding to be $2.33 \cdot 10^5$ sites/cell. Ouabain inhibition of (Na^+, K^+)-pump function was monitored by the cellular uptake of ^{86}Rb over 5 min. The larger fraction of ^{86}Rb uptake was ouabain sensitive and the ouabain concentration giving half-maximal inhibition was $2 \cdot 10^{-7}$ M. The cellular distribution of the ($Na^+ + K^+$)-ATPase was investigated using [^{3}H]ouabain autoradiography of intact freeze-dried epithelial monolayers of MDCK cells grown upon millipore filter supports. Binding of [^{3}H]ouabain is localised over the lateral cellular membranes. Autoradiogaphic silver grain density is close to background levels over both the apical and basal (attachment) membranes.

Introduction

Epithelial cells from various organs form sheets of cells in culture which retain certain structural and functional characteristics similar to their tissue of origin [1–4]. The dog kidney cell-line, MDCK, possesses a typical epithelial structure and demonstrates a small net transepithelial flux of Na^+ when grown upon permeable filter substrates [2–5]. These findings imply that there is a cellular polarity in the distribution of pump and leak pathways for ions as is found in natural epithelia [6–8]. In particular, the ($Na^+ + K^+$)-ATPase should be preferentially concentrated in the basal-lateral membranes of the MDCK cells [6–8].

The present paper is a study of the cellular distribution of the ($Na^+ + K^+$)-ATPase visualised using [^{3}H]ouabain autoradiography [6–8] in functional epithelial monolayers of dog kidney cells grown upon Millipore ® filter substrates.

The major finding is that the distribution of (Na^+, K^+)-pumps over the plasma membrane of intact MDCK cells is indeed non-uniform; autoradiographic silver grain density is close to background levels over the apical cellular membrane but is elevated 40-fold above background, over the lateral cellular membranes.

Materials and Methods

(i) Cell culture. MDCK renal epithelial cells at 60 serial passages (Flow Laboratories) were grown as described in Ref. 16. Cell monolayers were prepared upon 2.5 cm diameter Millipore ® filters (0.22 μm pore diameter) by seeding at high density [16] followed by growth to confluency (3–4 days). The formation of functional epithelial layers was monitored in cell monolayers from each batch by measuring electrical resistance and active transport potential [16].

(ii) Measurement of [^{3}H]ouabain binding and ^{86}Rb uptake. Ouabain and other cardiac glycosides

0 005-2736/81/0000–0000/$02.50

are specific inhibitors of the $(Na^+ + K^+)$-ATPase [9,10]. Interaction of ouabain with the $(Na^+ + K^+)$-ATPase is described by a simple reversible equilibrium [9,10]. [^{3}H]Ouabain may be utilised to count the cellular density of (Na^+, K^+)-pumps, 'specific binding' to the $(Na^+ + K^+)$-ATPase is estimated as the difference in binding between a pump conformation of high affinity in K^+-free media and a pump conformation of low affinity in a high K^+ (15 mM) media [9]. [^{3}H]Ouabain binding was determined upon MDCK cells grown to sub-confluency upon plastic petri dishes [11]; in brief, dishes were washed four times in Krebs solution [11] at 37°C; Krebs solution plus [^{3}H]ouabain was then added to the plates for 20 min incubation at 37°C. Unbound ouabain was removed by washing (four times in Krebs solution at 0°C for 1 min). Ice-cold wash media were employed to ensure that no loss of bound ouabain occurred. On the basis of [^{3}H]ouabain affinity and the rate of association of [^{3}H]ouabain specifically bound to the $(Na^+ + K^+)$-ATPase loss of ouabain in cold washes is extremely unlikely over the time employed. The washing protocol removed all of an extracellular space marker ([^{3}H]inulin) in separate experiments (preincubation was for 10 min at 37°C in Krebs solution). Cell numbers and volumes were measured directly by releasing cells by trypsin EDTA and counting using a Coulter Counter [12]. ^{86}Rb was used to trace for transmembrane uptake of K^+ [12]. The uptake of ^{86}Rb is linear with incubations up to 10 min. A 5-min incubation was standard. Monolayers were preincubated with ouabain at appropriate concentrations for 20 min in K^+-free Krebs solution; otherwise the protocol is similar to that for [^{3}H]ouabain binding [12]. ^{3}H-activity was counted by its β-emissions in a Packard liquid scintillation spectrometer; ^{86}Rb was counted by its Cerenkov emissions in the same spectrometer.

(iii) Autoradiography. Cell cultures grown as epithelial layers upon Millipore filters were washed four times in Krebs solution. [^{3}H]Ouabain was then added (12.5 μCi/cm^3, final ouabain concentration $2.5 \cdot 10^{-7}$ M) for 20 min at 37°C, in K^+-free or 15 mM K^+-containing Krebs solution. Unbound [^{3}H]-ouabain was removed by washing as above. Epithelial monolayers were then frozen in liquid propane cooled to liquid N_2 temperature (−185°C), transferred to liquid N_2 cooled containers and finally placed in an LFD1 freeze-drier (Nanotech. Instruments, U.K.). Freeze-drying was at $4 \cdot 10^{-6}$ torr for 116 h at temperatures from −88°C in 10 or 20 degrees Celsius steps to room temperature. Fixation was under vacuum in OsO_4 [6]. Monolayers were then enbedded in Araldite. Semi-thin sections (1 μm) were cut using a Phillips OmU_2 ultramicrotome and mounted on gelatin/chrome alum coated slides, covered with Kodak AR10 stripping film and exposed, dessicated, at 4°C in the dark for up to four weeks.

Autoradiographs were developed using Kodak D19 developer; sections were stained in Basic fuchsin and viewed under oil (X60 or X95 Leitz ultrapak objectives). Incident illumination was with a Leitz ortholux system. (Appropriate controls were run for latent image fading). Analysis of grain density was made from photographs using a summagraphics digitising tablet interfacted with an Olivetti P6060 minicomputer.

(iv) Electron microscopy. Cell monolayers were conventionally fixed and embedded in Araldite as described in Ref. 16. Thin sections were cut using a Phillips OmU_2 microtome, stained with lead acetate and uranyl acetate and viewed in a Phillips EM301 at an accelerating voltage of 60 kV.

Cell membrane perimeters were also measured using the Summagraphics digitising tablet/Olivetti P6060 computer from electron micrographs of thin sections of araldite embedded cell monolayers.

(v) Chemicals. All reagents were of Analar grade. Ouabain was obtained from the Sigma Chemical Company, Poole, Dorset. [^{3}H]Ouabain was obtained from the Radiochemical Centre, Amersham, U.K. Tissue culture supplies were obtained from Flow Laboratories, Irvine, Scotland and stripping film and developer from Kodak Ltd., Wythernshaw, Manchester, U.K.

Results

(a) Kinetics of [^{3}H]ouabain binding to intact MDCK cells

Figs. 1 and 2 show the concentration and time dependence of [^{3}H]ouabain binding to intact MDCK cells. Equilibrium values of 'specific' binding (the difference between K^+-free and 15 mM K^+-containing media) were observed at 20 min for $1 \cdot 10^{-6}$ and

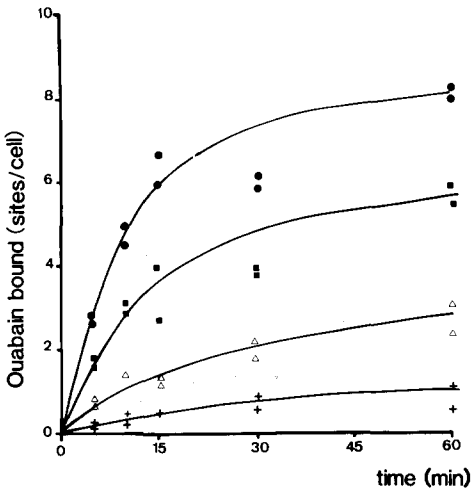

Fig. 1. Time dependence of [^{3}H]ouabain binding to intact MDCK cells. Data are taken from a single representative experiment. •, K^+-free media, $1 \cdot 10^{-6}$ M ouabain; ▪, 15 mM K^+-containing media, $1 \cdot 10^{-6}$ M ouabain; △, K^+-free media, $1 \cdot 10^{-7}$ M ouabain; +, 15 mM K^+-containing media, $1 \cdot 10^{-7}$ M ouabain.

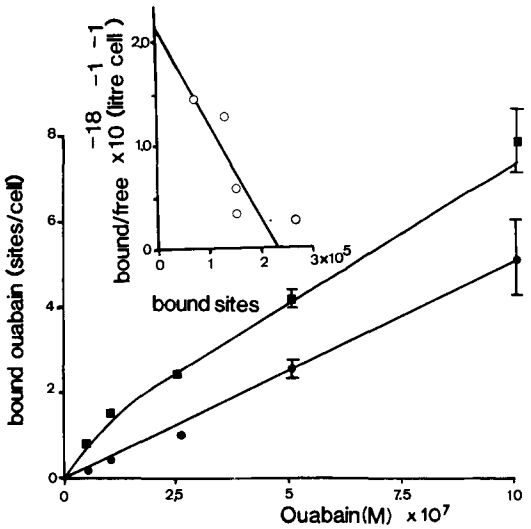

Fig. 2. Concentration dependence of [^{3}H]ouabain binding to intact MDCK cells. Incubations were for 20 min at 37°C. Each point represents the mean ± S.E. of four determinations; where not shown error bars lie within the points. ▪, K^+-free media; •, 15 mM K^+-containing media. The inset shows a Scatchard plot of specific ouabain binding. The solid-line was obtained by least-squares linear regression analysis (correlation coefficient r = 0.76, 20 degress of freedom, $P <$ 0.01).

$1 \cdot 10^{-7}$ M ouabain (Fig. 1). Binding in the presence of high K^+ (15 mM) media was a linear function of concentration (Fig. 2). Half-maximal specific binding is observed at 1.0 ± 0.5 (S.E.) $\cdot 10^{-7}$ M ouabain and the maximal binding of ouabain is 2.33 ± 0.45 (S.E.) $\cdot 10^5$ sites/cell. (Values derived from a Scatchard plot of specific binding from Fig. 2). This latter value is similar to HeLa cells $(0.5–1.0) \cdot 10^6$ sites/cell) and contrasts with the large amount of [^{3}H]ouabain binding reported by Cereijido et al. [13] for 110 passage MDCK cells.

(b) Inhibition of ^{86}Rb uptake by ouabain

Fig. 3 shows the effect of ouabain upon the activity of the $(Na^+ + K^+)$-ATPase monitored by cellular ^{86}Rb uptake. A large proportion of the Rb uptake is inhibited by ouabain; the ouabain-insensitive flux represents the passive transmembrane exchange of ^{86}Rb. Half-maximal inhibition by ouabain is observed at 2.08 ± 1.5 (S.E.) $\cdot 10^{-7}$ (data from the Hofstee plot). Taken together the [^{3}H]ouabain binding and ^{86}Rb-flux data are consistent with a nomal action of

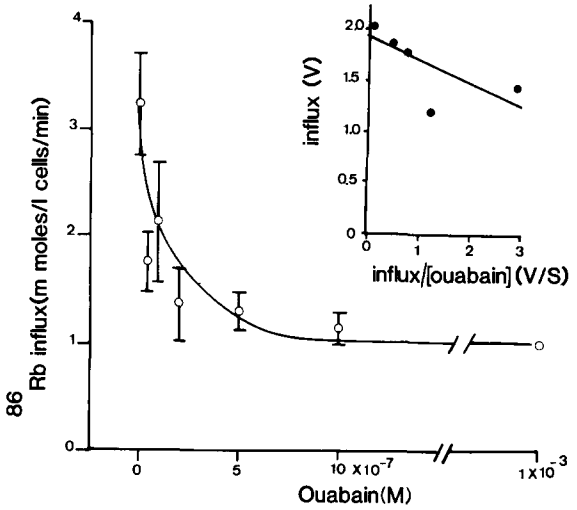

Fig. 3. Inhibition of ^{86}Rb uptake into MDCK cells by ouabain. Each point is the mean ± S.E. of four determinations. Where not shown error bars lie within the point. The inset shows a Hofstee plot of the ^{86}Rb-data corrected for the ouabain-insensitive ^{86}Rb influx at 1 mM ouabain. ^{86}Rb influx (v) (mmol/l cells/min) is plotted against the ^{86}Rb influx divided by the ouabain concentration (v/s) ($\times 10^4$, min^{-1}). The solid line represents the least-squares linear regression line (correlation coefficient r = 0.614, $P <$ 0.01, 20 degrees of freedom).

ouabain, namely a specific inhibitory action of ouabain upon the $(Na^+ + K^+)$-ATPase at the plasma membrane. Binding conditions for autoradiography to ensure maximal discrimination between 'specific' and 'non-specific' [^{3}H]ouabain binding were a ouabain concentration of $2.5 \cdot 10^{-7}$ M, and total incubation time of 20 min.

(c) Autoradiographic localisation

Fig. 4 shows the localisation of autoradiographic grains over an MDCK epithelial layer treated with [^{3}H]ouabain in a K^+-free medium. Prominent nuclei are visible under bright field illumination (Fig. 4B) which allows an unambiguous interpretation when the cell-layer is viewed with incident illumination (Fig. 4A). Autoradiograph grains are absent from cell nuclei and localised exclusively in the region of the cellular interspaces; they are virtually absent from either the apical region of the plasma membrane, or from the basal membranes adjacent to the Millipore filter. This view is substantiated by a statistical analysis of grain density over the interspace areas, apical membranes and basal membranes (Table I) taking 2-μm wide areas at each side of the three membranes of interest (cross-over points being ignored). Grain density is at least 40-fold higher in lateral-space areas than comparable apical or basal regions. Furthermore, grain density observed in the 4-μm sections over apical and basal areas does not differ significantly ($P < 0.5$, $P < 0.5$) from that observed in control areas in the same autoradiographs (Araldite and Millipore filter, respectively).

The high grain density over the lateral spaces is sensitive to incubation in high K^+ (15 mM)-containing media. Grain density is reduced from 13.06 ± 1.5 (S.E., $n = 78$ cells) grains/interspace in K^+-free media to 6.47 ± 0.3 (S.E., $n = 91$ cells) in 15 mM K^+-containing media. This result is in agreement with the observed effect of high K^+ media upon [^{3}H]ouabain binding in cells upon plastic substrates (see above) and is consistent with the high density of silver grains in the interspace region resulting from a specific association with the $(Na^+ + K^+)$-ATPase.

Calculation of the number of $(Na^+ + K^+)$-ATPase sites/cell from the observed 'specific' autoradiographic silver grain density (assuming (a) that β-emissions from only the surface 0.1 μm of the Araldite section activate silver grains, (b) that 50% of emissions are directed away from the nuclear film and (c) that the efficiency of the nuclear ARIO film is approx. 60% [14,15]) gives $2 \cdot 10^5$ sites/cell in agreement with the direct determinations made upon [^{3}H]ouabain binding upon MDCK cells (see above). Although the error involved in such calculations is

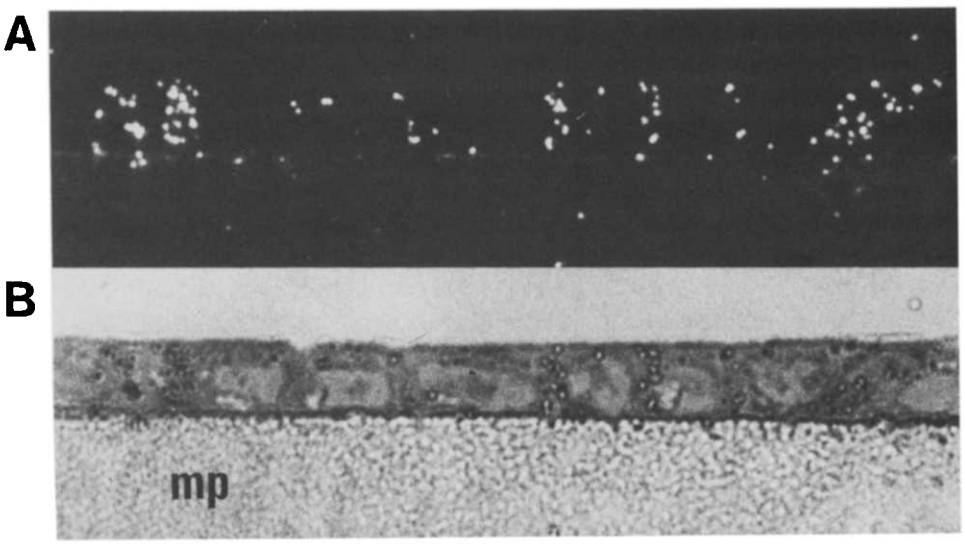

Fig. 4. Autoradiography of a single freeze-dried MDCK epithelial layer viewed under (A) incident dark-ground illumination, (B) transmitted bright-field illumination. mp, Millipore filter. Magnification:X1600.

TABLE I

ANALYSIS OF THE DISTRIBUTION OF [^{3}H]OUABAIN AUTORADIOGRAPHIC GRAINS IN THE MDCK MONOLAYER

Results are from digitised records of 33 cells, from two preparations and expressed as the mean ± S.E. 2-μm wide areas were taken over each of the membranes of interest and cross-over regions were ignored

Area	Autoradiographic grain density (grains/μm^2)($\times 10^2$)
Lateral interspace	47.0 ± 5.5
Apical membrane	0.4 ± 0.1
Araldite	0.6 ± 0.1
Basal membranes	1.4 ± 0.3
Millipore filter	1.2 ± 0.1

large, this result suggests that the processing involved for the autoradiographic analysis does not alter the total specific ouabain binding present in the tissue.

To assign the observed silver grain density to the source structure in the autoradiographs, account must be taken of (a) the absolute resolving power of the technique and (b) the complexity of the structure thought to contain the ^{3}H-label. For a linear source of ^{3}H in a thick section of 0.5 to 1 μm, the half-distance in which 50% of silver grains will be contained is 0.35 μm using ARIO emulsion and D19 developer [14,15]. The lateral space width in high resistance monolayers of MDCK cells is 0.2 to 1 μm in width and is thus not easy to identify with light microscopy [5,16]; also the lateral spaces contain interdigitations and (Fig. 6) are often observed to run at acute angles from the apical surface in thin sections viewed under the electron microscope (Fig. 6) [5,16]. Direct measurement of the distribution of silver grains over each bounding membrane of the lateral space is therfore impossible. Fig. 5, however, shows a statistical analysis of silver grain density about maximum likelihood best fit lines [17] through each cluster of silver grains over an MDCK cell layer. 75.4% of all silver grains lie within 1.0 μm of the centre-line of each cluster of silver grains. Though there are uncertainties in this approach, this result is consistent with surface binding of [^{3}H]ouabain to lateral space membranes of 0.5 to 1 μm in width.

Silver grain density does not display any dependence upon the depth into the cell from the apical surface (Table II) (taking 1-μm sections of the digitized records) suggesting that the density of the ($Na^+ + K^+$)-ATPase within the lateral space membranes is homogeneous. A similar conclusion has been reached for rabbit gall-bladder [18].

The absence of silver grains compared with background over the basal attachment membrane (Table I)

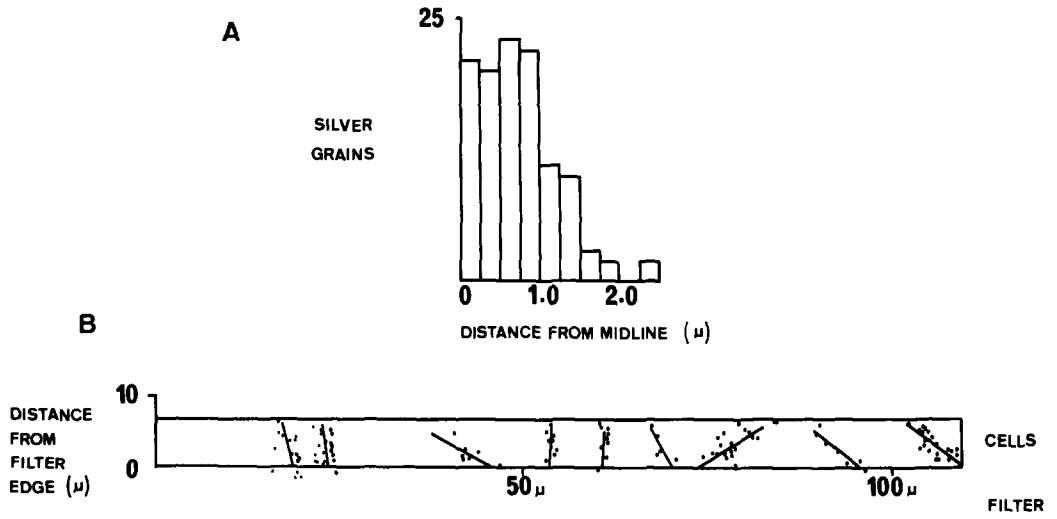

Fig. 5. Analysis of silver grain distribution (A) about maximum likelihood lines fitted to each cluster of silver grains over the lateral spaces (B).

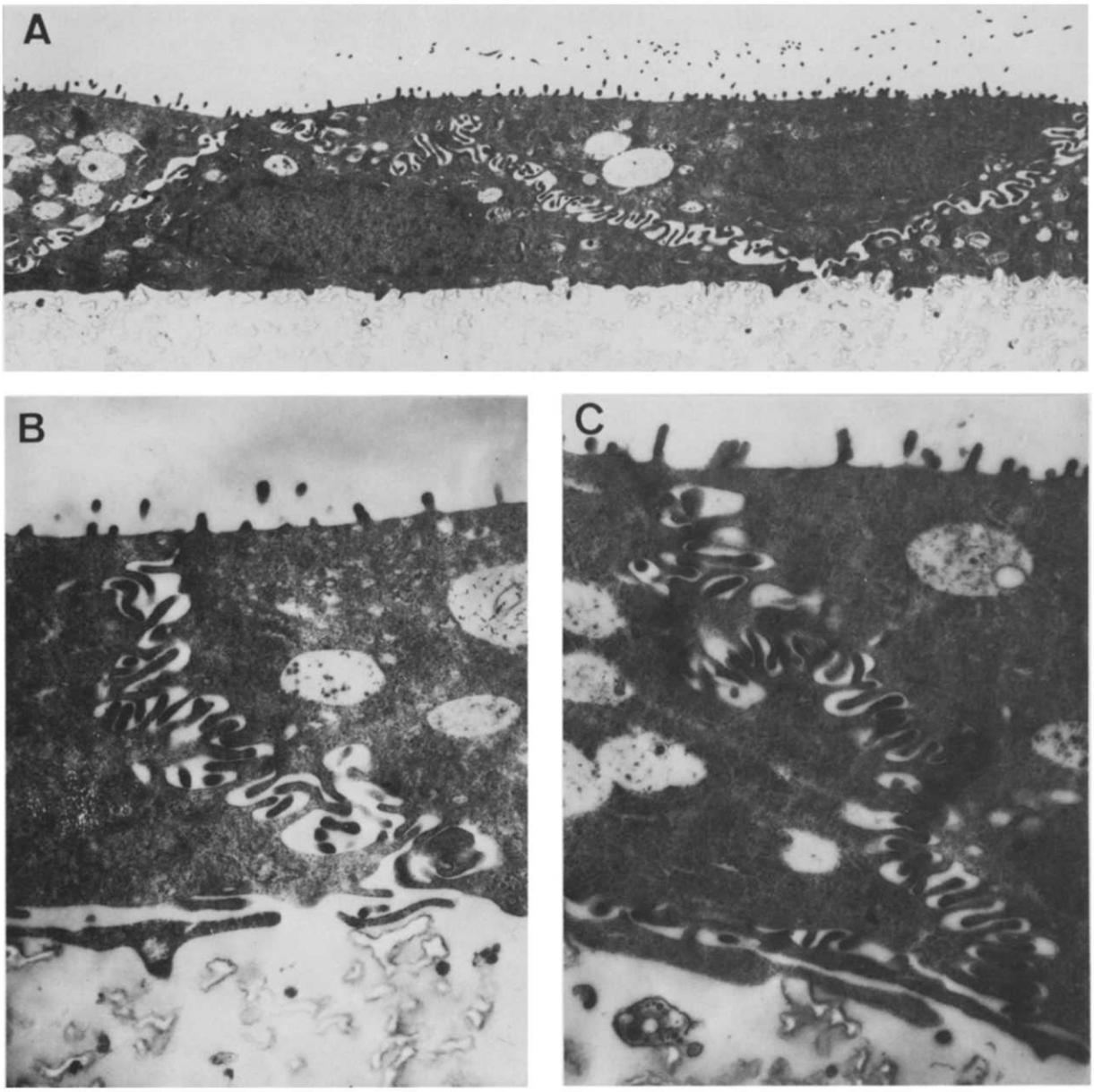

Fig. 6. Low power views of a confluent cell monolayer of 66 passage MDCK cells (A) (magnification: ×6210). (B) and (C) lateral cell spaces showing interdigitations (magnification:X16 380).

implies that the $(Na^+ + K^+)$-ATPase is not freely diffusible over the entire basal-lateral surface membranes. The heterogeneous distribution of silver grains over the basal-lateral membranes can not be explained by either differences in membrane area due to interdigitations within the lateral space or to restricted access of [^{3}H]ouabain to basal areas. The ratio of measured membrane perimeters in thin sections viewed by electron microscopy is, basal membrane 1.0, lateral space membranes 5.4 ± 0.76 (S.E., n = 8)

TABLE II

SILVER GRAIN DISTRIBUTION AS A FUNCTION OF DEPTH FROM THE APICAL SURFACE

Representative data is from digitised records of 10 cells

Distance from apical surface (μm)	Number of silver grains
0 –1.0	21
1.0–2.0	16
2.0–3.0	16
3.0–4.0	27
3.0–4.0	27
4.0–5.0	13

and apical membrane 1.4 ± 0.1 (S.E., $n = 8$). Colloidal La^{3+} perfused from the basal solution has also been observed to freely stain basal membranes in thin sections viewed in the electron microscope and to penetrate to the apical zonae occludentes (unpublished data). The absence of silver grains over the basal attachment membranes could also result from a chemical effect of the millipore substrate upon the nuclear film (negative chemography [15]); such an effect would be detected by a reduction in background grains over the whole millipore compared with the araldite background. No such reduction is observed (Table I). The heterogeneous distribution of Na^+-pumps observed here contradicts that of Louvard [19] who found an even staining of the basal-lateral membranes by the purified $(Na^+ + K^+)$-ATPase antibody of Kyte [20] in cells permeabilized by a freeze-thaw technique.

Discussion

Net ion transport across epithelial monolayers of MDCK cells requires a preferential localisation of the $(Na^+ + K^+)$-ATPase at the basal-lateral aspects of the cell layer. Previous studies have provided indirect evidence concerning the distribution of the $(Na^+ + K^+)$-ATPase in the MDCK cell [5,13]; binding of [^{3}H]ouabain from apical or basal surfaces of epithelial monolayers clamped in Ussing chambers has demonstrated a preferential binding of [^{3}H]ouabain to the basal surfaces of the cell layer [5,13]. In addition ouabain has been shown to inhibit the small spontaneous transepithelial electrical potential difference in high resistance monolayers only when applied to the basal bathing solution [5]. In this paper we provide direct evidence of the polarity in the distribution of the $(Na^+ + K^+)$-ATPase by using the technique of [^{3}H]ouabain autoradiography.

The validity of this technique is dependent upon the specificity to which ouabain binds to the $(Na^+ + K^+)$-ATPase. In other systems there is considerable evidence that ouabain binds with high affinity and specificity to a single site at the $(Na^+ + K^+)$-ATPase [9,10]. (Na^+, K^+)-pump function in MDCK cells as monitored by ^{86}Rb uptake is inhibited by ouabain with high affinity. Previously we have shown that ouabain reduces ATP hydrolysis in MDCK cell homogenates [16]. Additionally [^{3}H]ouabain binding to intact MDCK cells grown upon petri dishes displays characteristics similar to other intact cells [9,11,12]. In particular high K^+ media affects [^{3}H]-ouabain binding, probably due to a K^+-induced change in the affinity of the pump to ouabain [21,22]. The K^+ effect has also been used to estimate non-specific [^{3}H]ouabain binding [9,11,12] and provides an excellent control in regard to the specificity of labelling observed in the present autoradiographs [7,8].

Localisation of the $(Na^+ + K^+)$-ATPase to the lateral membrane area with a grain density over the apical membranes equivalent to background levels is in agreement with the net transepithelial ion transport in these cell layers [5]. The cellular polarity of the $(Na^+ + K^+)$-ATPase also emphasizes the extensive retention of differentiated structure and function in this established cell-line. An asymmetric Na^+-pump distribution has also recently been reported for the pig kidney cell-line $LLCPK_1$ [26].

The present results also suggest that the (Na^+, K^+)-pump density over the basal membranes is reduced compared to that expected of an even density of (Na^+, K^+)-pumps over the basal-lateral membrane area. Thus although a 5-fold higher pump density is expected in lateral space areas due to an increased membrane area resulting from interdigitations, a 40-fold higher density is observed. In natural epithelia where localisation of pump sites have been made, a comparison of (Na^+, K^+)-pump density over the basal membranes compared to that over the lateral membranes has not explicitly been dealt with [7,8,20] probably as a result of the extensive infoldings and the complex geometry of lateral spaces with com-

plicate interpretation [20]. In natural epithelia maintenance of the apical and basal-lateral membrane domains is thought to arise from apical junctional complexes preventing diffusion and intermixing of membrane compartments [23,24,25]. The present results imply that diffusion-restriction by the apical junctional complexes are not the only means by which the distribution of the $(Na^+ + K^+)$-ATPase over the surface plasma membranes of the MDCK cell is controlled. In a recent paper Louvard [19] has reported an even distribution of the $(Na^+ + K^+)$-ATPase over the basal-lateral membranes of MDCK cells using the antibody method of Kyte [20], this discrepancy with present results may be due to the use of a different cell-strain of MDCK [16] or may result from the freeze-thaw step used to permeabilize the cells to the anti-$(Na^+ + K^+)$-ATPase antibody which may affect cell structure.

The demonstration of the normal epithelial distribution of (Na^+, K^+)-pumps over the plasma membrane of MDCK cells further emphasizes the potential of the MDCK cell-line as a useful tissue culture model to study the establishment and maintenance of epithelial membrane domains [19].

Acknowledgments

This work was supported by a grant from the Wellcome Trust. We thank Dr. A.R. Chipperfield for comments on a preliminary draft of the paper. Professor R.M. Cormack gave valuable statistical advice.

References

1 Handler, J.S., Perkins, F.M. and Johnson, J.P. (1980) Am. J. Physiol. 238, F1–F9
2 Misfeldt, D.S., Hamamoto, S.T. and Pitelka, D.R. (1976) Proc. Natl. Acad. Sci. U.S.A. 73, 1212–1216
3 Cereijido, M., Robbins, E.S., Dolan, W.J., Rotunno, C.A. and Sabatini, D.D. (1978) J. Cell. Biol. 77, 853–880
4 Richardson, J.C.W. and Simmons, N.L. (1979) FEBS Lett. 105, 201–204
5 Simmons, N.L. (1981) J. Membrane Biol., in the press
6 Stirling, C.E. (1972) J. Cell. Biol. 533, 704–714
7 Dibona, D.R. and Mills, J.W. (1979) Fed. Proc. 38, 134–143
8 Quinton, P.M. and Tormey, John McD (1976) J. Membrane Biol. 29, 383–399
9 Baker, P.F. and Willis, J.S. (1972) J. Physiol. (Lond.) 224, 441–462
10 Glynn, I.M. and Karlish, S.J.D. (1975) Annu. Rev. Physiol. 37, 13–85
11 Boardman, L.J., Lamb, J.F. and McCall, D. (1972) J. Physiol. (Lond.) 255, 619–635
12 Boardman, L.J., Huett, M., Lamb, J.F., Newton, J.P. and Polson, J.M. (1974) J. Physiol. (Lond.) 241, 771–794
13 Cereijido, M., Enrenfeld, J., Meza, I., Martinez-Palomo, A. (1980) J. Membrane Biol. 52, 147–159
14 Hill, D.K. (1962) Nature 194, 831–832
15 Rogers, A.W. (1973) In Techniques in Autoradiography pp. 52–60, Elsevier Science Publishing Company New York
16 Richardson, J.C.W., Scalera, V. and Simmons, N.L. (1981) Biochim. Biophys. Acta 673, 26–36
17 Sprent, P. (1969) in Models in Regression and Related Topics, Methuen, London
18 Mills, J.W. and Dibona, D.R. (1978) Nature 271, 273–275
19 Louvard, D. (1980) Proc. Natl. Acad. Sci. U.S.A. 77, 4132–4136
20 Kyte, J. (1976) J. Cell. Biol. 68, 287–303
21 Chipperfield, A.R. and Whittam, R. (1973) Nature 242, 62–63
22 Erdman, E. and Schoner, W. (1973) Biochim. Biophys. Acta 330, 302–318
23 Kinne, R. (1976) Curr. Top. Membrane. Trans. 8, 209–267
24 Pisam, M. and Ripoche, P. (1976) J. Cell. Biol. 71, 907–920
25 Galli, P., Brenna, A., De Camilli, P. and Meldolesi, J. (1976) J. Expl. Cell. Res. 178–183
26 Mills, J.W., Macknight, A.D.C., Dayer, J.M. and Ausiello, D.A. (1979) Am. J. Physiol. 236, 157–162